Available online at www.eccomasproceedia.org
Eccomas Proceedia SMART (2023) 1161-1172

ECCOMAS
Proceedia

X ECCOMAS Thematic Conference on Smart Structures and Materials
SMART 2023
D.A. Saravanos, A. Benjeddou, N. Chrysochoidis and T. Theodosiou (Eds)

A FAST IDENTIFICATION ALGORITHM FOR LINEAR PARAMETER VARYING VECTOR AR MODELS OF SHORT-TERM DRIVETRAIN VIBRATION

Luis David Avendaño-Valencia[a] **and Andriana S. Georgantopoulou**[b]

[a] Department of Mechanical and Electrical Engineering
University of Southern Denmark (SDU)
Campusvej 55, 5230 Odense, Denmark
e-mail: ldav@sdu.dk

[b] Master in Mechanical Engineering
University of Aarhus
e-mail: andgeorgant@gmail.com

Key words: Wind turbine drivetrain, drivetrain vibration, condition monitoring, linear parameter varying models

Abstract. Wind turbine drivetrain vibrations are characterised by very complex dynamics originating from the convolution of deterministic and stochastic excitation sources moving through the structural dynamics of the wind turbine. In this work we postulate Linear Parameter Varying Vector AutoRegressive (LPV-VAR) models to represent those signals. To deal with the complexity of these models during the identification procedure, we devise an algorithm, based on the QR decomposition of the regression matrix, to accelerate the model identification procedure. The proposed methods are demonstrated on data from a wind turbine drivetrain simulator.

1 INTRODUCTION

Wind turbine drivetrains are subject to continuous loads over extended periods of time in a demanding operational environment. As a result, these components are highly exposed to fatigue and damage. The unrelenting requirement for permanent availability elevates the cost of maintenance and repairs, which calls for effective ways to keep them operating [1, 2]. Among other technologies, vibration-based *Condition Monitoring* (CM) is of great interest for health assessment of wind turbine drivetrains.

In the development of vibration-based CM methods, it is necessary to deal with the high complexity of the signals originating from drivetrains. Classically, vibration from rotating machines is considered to result from [3, Sec. 1.7]: (i) deterministic sources, mainly related to the rotation of the machine itself, and distinguished as harmonics dominating the vibration response; (ii) stochastic sources, related to background random excitation that originates, for instance, from the contact between moving surfaces. All these sources are convoluted through the structural

Peer-review under responsibility of the organizing committee of SMART 2023.
doi: 10.7712/150123.9865.451289

dynamics of the machine, creating the complex vibration signals that are measured from the machine. Moreover, the dynamic features of different damage types add up to the already complex vibration characteristics of a drivetrain.

It is usual to separate deterministic and stochastic sources for independent analysis within damage diagnosis procedures [4]. Typical methods include cepstral editing, wavelet and other signal decompositions, like the empirical mode decomposition [1, 2, 4]. Supervised methods can also be used to guide the signal decomposition or feature extraction procedure [5]. Among these, complex algorithms powered by deep learning, are used to extract damage sensitive features from raw vibration signals for specific damage types [6]. For this purpose, large vibration datasets from healthy and target damage conditions across several operational conditions are usually required. The success of these techniques is bound to the thoroughness of the dataset, especially regarding to the abundance of operational conditions that can guarantee the generalisation capability of the feature extraction procedures [7]. This has been proven to be challenging, particularly when considering real-life damages.

An alternative approach is to train a model to represent the global dynamics of the structure. Such model could be used as a surrogate for the real structure in a reference health condition and for comparison with the present state of the machine [8, 9]. In the case of rotating machines, the main challenge is to devise a simple modelling methodology regardless of the complexity of the vibration response signals. Various time-series modelling methods have emerged, based on time-varying, parameter-varying or non-linear Auto-Regressive modelling [10, 11, 12]. In particular, the *Linear-Parameter-Varying* (LPV) approach can potentially provide efficient representations of the dynamics of rotating machines as a function of a reference shaft angle, and other operational variables. Nonetheless, these models quickly grow in complexity, according to the number of concurrent vibration signals and scheduling variables, which challenges conventional identification procedures and practical usability.

Our main objective is to develop a *global modelling* approach for the vibration response of wind turbine drivetrains, considering the machine's rotational dynamics over a range of operational set points. As part of that objective, in this work, we postulate *Linear Parameter Varying Vector Auto-Regressive* (LPV-VAR) models to achieve compact, accurate, efficient, and explainable representations of drivetrain vibration response at multiple measurement points (sensors). More specifically, in this work we focus on the application of LPV-VAR models to represent the vector vibration response of the drivetrain, using the (instantaneous) shaft angle as scheduling variable, while the shaft speed (RPM) and load are kept fixed. The global dynamics, considering a range of operational set points (speed and load), is considered in an upcoming publication.

As the complex machine dynamics call for high-complexity models, we design an efficient algorithm based on the QR decomposition of the regression matrix, which speeds up the model complexity selection. The latter may be regarded as the main contribution of this work. Moreover, we use the periodic-basis LPV-VAR models to calculate frequency-domain and time-frequency characteristics of the vibration response, which is helpful for assessment of different health conditions. In the same way, we are able to demonstrate that the periodic basis facilitates the representation of the harmonics in the spectra of vibration signals. The proposed methods are demonstrated on vibration data from a wind turbine drivetrain simulator, characterised by three shafts and two speed reduction gearboxes, where the speed and load torque may be controlled. Here, we consider the vibration response of the test rig for fixed speed and load on a pair of

sensors located on one of the drivetrain bearings. The proposed methodology is presented in Sec. 2, the experimental set-up and analysis results are presented in Sec. 3. Conclusions of this study along with upcoming research perspectives are presented in Sec. 4.

2 METHODOLOGY

2.1 Linear Parameter Varying VAR Modelling of Short-Term Dynamics

Here, we consider the short-term modelling of the vibration response of the parameter varying system, noted as $\boldsymbol{y}[t] \in \mathbb{R}^n$, where n indicates the number of concurrent signals. The instantaneous dynamics of the system are governed by a synchronous *scheduling variable* $\beta[t] \in \mathbb{R}$. In the short-term analysis considered here, we assume that the system is set on a fixed operating point, determined by the vector $\boldsymbol{\xi} \in \mathbb{R}^m$. In the context of a wind turbine drivetrain, the scheduling variable corresponds to a reference shaft angle, while the set point vector comprises the reference shaft speed and drivetrain load. Time-domain modelling of the response signal is then performed via the LPV-VAR model [9, 8]:

$$\boldsymbol{y}[t] = -\sum_{i=1}^{n_a} \boldsymbol{A}_i(\beta[t-i]) \cdot \boldsymbol{y}[t-i] + \boldsymbol{\varepsilon}[t] \quad , \quad \boldsymbol{\varepsilon}[t] \sim \mathcal{N}\left(\boldsymbol{0}, \boldsymbol{\Sigma}_{\boldsymbol{\varepsilon}}\right) \tag{1a}$$

$$\boldsymbol{A}_i(\beta[t]) = \sum_{j=1}^{p_a} \boldsymbol{A}_{i,j} \cdot G_{b_{a(j)}}(\beta[t]) \quad , \quad \mathcal{F}_{\mathrm{AR}} = \left\{ G_{b_{a(j)}}(\beta[t]), \ldots, G_{b_{a(p_a)}}(\beta[t]) \right\} \tag{1b}$$

where n_a is the AR order, p_a the basis order, $\beta[t] \in \mathbb{R}$ the scheduling variable, $\boldsymbol{A}_i(\beta[t]) \in \mathbb{R}^{n \times n}$ the AR parameter matrices as a function of the scheduling variable, $\boldsymbol{\varepsilon}[t] \in \mathbb{R}^n$ is a zero-mean *Normally and Independently Distributed* (NID) innovations with covariance matrix $\boldsymbol{\Sigma}_{\varepsilon} \in \mathbb{R}^{n \times n}$, and lastly, $\mathcal{F}_{\mathrm{AR}}$ is a function subspace that includes the chosen basis vector with indices indicated by the vector $\boldsymbol{b}_a := \begin{bmatrix} b_{a(1)} & b_{a(2)} & \cdots & b_{a(p_a)} \end{bmatrix}^T$. The LPV-VAR model can be cast into the following regression form, which is the basis for estimation [9, 8]:

$$\boldsymbol{y}[t] = \boldsymbol{\Theta} \cdot \boldsymbol{\phi}[t] + \boldsymbol{\varepsilon}[t] \tag{2a}$$

$$\boldsymbol{\Theta} = \begin{bmatrix} \boldsymbol{A}_{1,1} & \cdots & \boldsymbol{A}_{1,p_a} & \cdots & \boldsymbol{A}_{n_a,1} & \cdots & \boldsymbol{A}_{n_a,p_a} \end{bmatrix} \quad , \quad \boldsymbol{\phi}[t] = \begin{bmatrix} \boldsymbol{g}(\beta[t-1]) \otimes \boldsymbol{y}[t-1] \\ \vdots \\ \boldsymbol{g}(\beta[t-n_a]) \otimes \boldsymbol{y}[t-n_a] \end{bmatrix} \tag{2b}$$

where $\boldsymbol{\Theta} \in \mathbb{R}^{n \times d}$, with $d = n \cdot n_a \cdot p_a$, is the model coefficient matrix, $\boldsymbol{\phi}[t] \in \mathbb{R}^d$ is the regression vector, $\boldsymbol{g}(\beta[t]) = \begin{bmatrix} G_{b_a(1)}(\beta[t]) & \cdots & G_{b_a(p_a)}(\beta[t]) \end{bmatrix}^T \in \mathbb{R}^{p_a}$ is the basis function vector, and $\otimes$ indicates the Kronecker (tensor) product.

In the context of modelling the vibration response of rotating machines, the scheduling variable $\beta[t] \in [0, 1]$ is selected as the normalised shaft angle, where 1 indicates a full revolution. Accordingly, the functional expansion basis is selected as the Fourier basis, defined as:

$$G_0(\beta[t]) = 1 \qquad G_{2j-1}(\beta[t]) = \sin j2\pi\beta[t] \qquad G_{2j}(\beta[t]) = \cos j2\pi\beta[t] \tag{3}$$

with $j = 1, \ldots, (p_a - 1)/2$. Note that to preserve the balance between the number of sines and cosines, the basis order p_a should be an odd number. In general, it is possible to use other types

of periodic expansion basis to represent vibration of rotating machines, but as will be shown in the sequel, it is very convenient to use the Fourier basis, as it can be readily used to calculate spectral correlation functions and time-dependent spectra [13, Ch. 4].

2.2 LPV-VAR model identification procedure

Model estimation is based on an N-length response signal, $\boldsymbol{y}[t]$ with $t = 1, 2, \ldots, N$, with the corresponding scheduling variable $\beta[t]$. Model identification then involves estimation of the model parameter matrix $\boldsymbol{\Theta}$ and innovations covariance $\boldsymbol{\Sigma_w}$, and the selection of the structural parameters n_a and p_a. A brief description based on a conventional *Maximum Likelihood* (ML) setting is provided below, which follows from the developments in [8].

ML parameter estimation Based on the regression form or the LPV-VAR model we can construct the matrix of predicted responses for the analysis period, as follows:

$$\boldsymbol{Y} = \boldsymbol{\Theta} \cdot \boldsymbol{\Phi} + \boldsymbol{E} = \hat{\boldsymbol{Y}} + \boldsymbol{E} \tag{4}$$

where $\hat{\boldsymbol{Y}} := \boldsymbol{\Theta} \cdot \boldsymbol{\Phi}$ is the matrix of the LPV-VAR model *one-step-ahead predictions*, with:

$$\boldsymbol{Y} := \begin{bmatrix} \boldsymbol{y}[n_a+1] & \boldsymbol{y}[n_a+2] & \cdots & \boldsymbol{y}[N] \end{bmatrix}_{n \times (N-n_a)} \tag{5a}$$

$$\boldsymbol{\Phi} := \begin{bmatrix} \boldsymbol{\phi}[n_a+1] & \boldsymbol{\phi}[n_a+2] & \cdots & \boldsymbol{\phi}[N] \end{bmatrix}_{d \times (N-n_a)} \tag{5b}$$

$$\boldsymbol{E} := \begin{bmatrix} \boldsymbol{\varepsilon}[n_a+1] & \boldsymbol{\varepsilon}[n_a+2] & \cdots & \boldsymbol{\varepsilon}[N] \end{bmatrix}_{n \times (N-n_a)} \tag{5c}$$

Following from the NID innovations, the response matrix $\boldsymbol{Y}$ can be associated with a matrix-normal distribution[1] defining the model's likelihood, as:

$$p(\boldsymbol{Y} \,|\, \boldsymbol{\Phi}, \boldsymbol{\Theta}, \boldsymbol{\Sigma_\varepsilon}) = \mathcal{MN}(\hat{\boldsymbol{Y}}, \boldsymbol{\Sigma_\varepsilon}, \boldsymbol{I}_{N-n_a}) \tag{6}$$

with mean $\hat{\boldsymbol{Y}}$, *row-space* (responses) covariance matrix $\boldsymbol{\Sigma_\varepsilon}$, and *column-space* (time-instances) covariance matrix equal to the identity matrix $\boldsymbol{I}_{N-n_a}$ of dimension $N - n_a$. Conventional *Maximum Likelihood* (ML) estimates of the parameter matrix and innovations covariance – equivalent to the *Ordinary Least Squares* (OLS) estimates– can be calculated as the values maximising Eq. (6), which yields [8]:

$$\hat{\boldsymbol{\Theta}}_{\mathrm{ML}} = \boldsymbol{Y} \cdot \boldsymbol{\Phi}^T \cdot (\boldsymbol{\Phi} \cdot \boldsymbol{\Phi}^T)^{-1}, \qquad \hat{\boldsymbol{\Sigma}}_{\boldsymbol{\varepsilon}} = \frac{1}{N - n_a} (\boldsymbol{Y} - \hat{\boldsymbol{\Theta}}_{\mathrm{ML}} \cdot \boldsymbol{\Phi})(\boldsymbol{Y} - \hat{\boldsymbol{\Theta}}_{\mathrm{ML}} \cdot \boldsymbol{\Phi})^T \tag{7}$$

Resulting from the matrix-normal likelihood, the distribution of the parameter matrix conditional to the available data also follows a matrix-normal distribution[2], defined as:

$$p(\boldsymbol{\Theta} \,|\, \boldsymbol{Y}, \boldsymbol{\Phi}, \boldsymbol{\Sigma_\varepsilon}) = \mathcal{MN}(\hat{\boldsymbol{\Theta}}_{\mathrm{ML}}, \boldsymbol{\Sigma_\varepsilon}, \boldsymbol{\Lambda}_N^{-1}) \tag{8}$$

[1] A matrix-normal distribution, noted as $\mathcal{MN}(\boldsymbol{M}, \boldsymbol{\Sigma}_r, \boldsymbol{\Sigma}_c)$, with mean matrix $\boldsymbol{M} \in \mathbb{R}^{n_r \times n_c}$ and row and column covariance matrices $\boldsymbol{\Sigma}_r \in \mathbb{R}^{n_r \times n_r}$ and $\boldsymbol{\Sigma}_c \in \mathbb{R}^{n_c \times n_c}$ respectively, is equivalent to the multivariate normal distribution $\mathcal{N}(\mathrm{vec}(\boldsymbol{M}), \boldsymbol{\Sigma}_c \otimes \boldsymbol{\Sigma}_r)$, where $\mathrm{vec}(\boldsymbol{M})$ is the vectorisation operator, which stacks the columns of $\boldsymbol{M}$ into a single vector of size $n_r \cdot n_c$.

[2] This may be interpreted as the posterior parameter matrix distribution in a Bayesian perspective, and in fact arises from a non-informative prior for $\boldsymbol{\Theta}$ and deterministic $\boldsymbol{\Sigma_\varepsilon}$, according to the framework in [14, Sec. 2.8].

with mean $\hat{\boldsymbol{\Theta}}_{\mathrm{ML}}$ the ML estimate of the parameter matrix, $\boldsymbol{\Sigma}_{\boldsymbol{\varepsilon}} \in \mathbb{R}^{n\times n}$ the row-space (responses) covariance, and $\boldsymbol{\Lambda}_N^{-1} := (\boldsymbol{\Phi}\cdot\boldsymbol{\Phi}^T)^{-1} \in \mathbb{R}^{d\times d}$ the column-space (regressors) covariance.

The major computational load of the parameter estimation procedure comes from the calculation of the inverse of the matrix $\boldsymbol{\Lambda}_N$. Likewise, this operation is sensitive to numerical inconsistencies if the said matrix becomes ill-conditioned. Presently, that happens for (relatively) large model structures (as n_a, p_a become larger).

Model structure selection Model structure selection is conventionally performed by a discrete search on the space spanned by the model complexity parameters n_a and p_a. Accordingly, a range of values for n_a and p_a is initially selected, and models of different complexities are calculated within the range. Then, fit criteria, such as the *Residual Sum of Squares over the Series Sum of Squares* (RSS/SSS) or *Bayesian Information Criterion* (BIC) are used to guide the selection of the best fitting model structure [8]. This conventional procedure requires repeated model estimations, involving the calculation of the inverse of a regression matrix with increasing number of rows (regressors).

A computationally efficient implementation can be achieved with the help of the QR decomposition. To this end, we consider the QR decomposition of the transposed regression matrix $\boldsymbol{\Phi}^T = \boldsymbol{Q}\cdot\boldsymbol{R}$, where $\boldsymbol{Q} \in \mathbb{R}^{(N-n_a)\times d}$ is a matrix with orthogonal columns, so that $\boldsymbol{Q}^T\boldsymbol{Q} = \boldsymbol{I}_d$, and $\boldsymbol{R} \in \mathbb{R}^{d\times d}$ is a square upper triangular matrix. Using the QR decomposition, we can rewrite the ML parameter matrix estimator, as follows:

$$\hat{\boldsymbol{\Theta}}_{qr} = \boldsymbol{Y}\cdot\boldsymbol{Q}\cdot\boldsymbol{R}\cdot(\boldsymbol{R}^T\boldsymbol{Q}^T\boldsymbol{Q}\boldsymbol{R})^{-1} = \tilde{\boldsymbol{Y}}\boldsymbol{R}\cdot(\boldsymbol{R}^T\boldsymbol{R})^{-1} \tag{9}$$

where $\tilde{\boldsymbol{Y}} := \boldsymbol{Y}\cdot\boldsymbol{Q} \in \mathbb{R}^{n\times d}$ is the projection of the response matrix to the column space of $\boldsymbol{\Phi}$. Hence, we can interpret Eq. (9) as an equivalent regression of the projected response matrix $\tilde{\boldsymbol{Y}}$ on the regressors defined by the columns of matrix $\boldsymbol{R} = \begin{bmatrix}\boldsymbol{r}_1 & \boldsymbol{r}_2 & \cdots & \boldsymbol{r}_d\end{bmatrix}$.

Accordingly, fast calculation of individual model parameter estimates can be achieved using the alternative system of linear equations $\tilde{\boldsymbol{Y}} = \boldsymbol{\Theta}\boldsymbol{R}^T$, which can be easily solved by back-substitution, given the triangular nature of $\boldsymbol{R}$. This avoids direct calculation of the inverse in Eq. (9). Moreover, each one of the columns of $\boldsymbol{R}$ can be added sequentially, to obtain model estimates of increasing complexities. This has the same effect as adding individual regressors to the LPV-VAR model. Using these properties, the fast AR model order selection procedure in Tab. 1 is established. Note that the procedure can be easily modified to facilitate the selection of the basis order, p_a, by adequate selection of the indices of the $\boldsymbol{R}$ and $\boldsymbol{\Phi}$ matrices.

2.3 LPV-VAR model based analysis

The obtained LPV-VAR models can be used to obtain parametric estimates of frequency-domain and time-frequency characteristics of the underlying cyclo-stationary process. Here, we consider the Harmonic-FRF and time-varying spectra, briefly detailed below.

Harmonic-FRF The *Harmonic Frequency Response Function* (Harmonic-FRF) is a generalisation of the conventional FRF for Linear Time-Periodic (LTP) systems. With the Harmonic-FRF the response of the LTP system is represented as the sum of the responses of a bank of

1: **Given:** $\boldsymbol{y}[t] \in \mathbb{R}^n$, $t = 1, 2, \ldots, N$, n_a and p_a
2: $\boldsymbol{Y}, \boldsymbol{\Phi} \leftarrow$ BUILDMATRICES($\boldsymbol{y}[t]$,n_a,p_a) ▷ Build matrices $\boldsymbol{Y}$ and $\boldsymbol{\Phi}$ as in Eq. (5)
3: $\boldsymbol{Q}, \boldsymbol{R} \leftarrow \mathrm{QR}(\boldsymbol{\Phi}^T)$ ▷ Calculate QR decomposition
4: $\tilde{\boldsymbol{Y}} \leftarrow \boldsymbol{Y} \cdot \boldsymbol{Q}$ ▷ Project $\boldsymbol{Y}$ into column space of $\boldsymbol{\Phi}$
5: **for** $i = 1, \ldots, n_a$ **do**
6: SOLVE($\tilde{\boldsymbol{Y}} = \boldsymbol{\Theta}^{(i)} \cdot \begin{bmatrix} \boldsymbol{r}_1 & \boldsymbol{r}_2 & \cdots & \boldsymbol{r}_{i \cdot p_a} \end{bmatrix}^T$) ▷ Solve linear system for AR order i
7: $\boldsymbol{E} \leftarrow \boldsymbol{Y} - \boldsymbol{\Theta}^{(i)} \cdot \left[\boldsymbol{\Phi}\right]_{1:i \cdot p_a}$ ▷ Calculate prediction error
8: rss_sss[i], bic[i] $\leftarrow$ FITCRITERIA($\boldsymbol{E}$) ▷ Calculate fit criteria
9: **end for**
10: $n_{a(opt)} \leftarrow$ FINDMIN(rss_sss,bic)

$\left[\boldsymbol{\Phi}\right]_{1:i \cdot p_a}$ indicates the first $i \cdot p_a$ rows (regressors) of the regression matrix $\boldsymbol{\Phi}$

Table 1: Fast algorithm for model order selection of LPV-VAR models.

filters fed by frequency-shifted versions of the excitation. In formal terms, this relation writes as follows [13, Ch. 4]:

$$Y(\omega) = \sum_{k=-n_h}^{n_h} \breve{H}_k(\omega) \cdot X(\omega - k\Omega) = \breve{\boldsymbol{H}}^T(\omega) \cdot \breve{\boldsymbol{X}}(\omega) \tag{10}$$

where $X(\omega)$ and $Y(\omega)$ indicate the DFT of the excitation and response, correspondingly, and:

$$\breve{\boldsymbol{H}}(\omega) = \begin{bmatrix} \breve{H}_{-n_h}(\omega) & \breve{H}_{-1}(\omega) & \breve{H}_0(\omega) & \breve{H}_1(\omega) & \cdots & \breve{H}_{n_h}(\omega) \end{bmatrix}^T$$
$$\breve{\boldsymbol{X}}(\omega) = \begin{bmatrix} X(\omega + n_h\Omega) & \cdots & X(\omega + \Omega) & X(\omega) & X(\omega - \Omega) & \cdots & X(\omega - n_h\Omega) \end{bmatrix}^T$$

The Harmonic-FRF then corresponds to the functions $\breve{H}_k(\omega) \in \mathbb{C}$, $k = [-n_h, \ldots, n_h]$, which are interpreted as the FRF of each one of the individual filters making up the response. For the LPV-VAR model of Eq. (1), the Harmonic-FRF vector $\breve{\boldsymbol{H}}(\omega)$, can be calculated as [13, Ch. 4]:

$$\breve{\boldsymbol{H}}(\omega) = \left(\boldsymbol{I} + \sum_{i=1}^{n_a} \mathrm{e}^{-j\omega T_s i} \cdot \boldsymbol{\Omega}^{-i} \cdot \breve{\boldsymbol{A}}_i \right)^{-1} \cdot \breve{\boldsymbol{c}}_o \tag{11}$$

$$\breve{\boldsymbol{A}}_i = \begin{bmatrix} \breve{a}_i[0] & \breve{a}_i[-1] & \cdots & \breve{a}_i[-n_h] \\ \breve{a}_i[1] & \breve{a}_i[0] & \cdots & \breve{a}_i[-n_h + 1] \\ \vdots & \vdots & \ddots & \vdots \\ \breve{a}_i[n_h] & \breve{a}_i[n_h - 1] & \cdots & \breve{a}_i[0] \end{bmatrix}_{(2n_h+1)\times(2n_h+1)} \qquad \breve{\boldsymbol{c}}_o = \begin{bmatrix} 0 \\ \vdots \\ 0 \\ 1 \\ 0 \\ \vdots \\ 0 \end{bmatrix}_{2n_h+1}$$

where $\breve{\boldsymbol{A}}_i$ is a circulant matrix with the DFT coefficients of the LPV-VAR model parameters $\breve{a}_i[k] \in \mathbb{C}$ for a number of harmonics n_h of a reference shaft, $\boldsymbol{\Omega} = \mathrm{diag}(\exp(-j\mathbf{k}\Omega T_s))$ is a diagonal complex exponential matrix evaluated on the harmonics indicated by the vector $\mathbf{k} =$

$\begin{bmatrix}-n_h & \cdots & -1 & 0 & 1 & \cdots & n_h\end{bmatrix}$, and Ω is the reference shaft speed, in rad/s. In the case of the LP-VAR model with Fourier basis, the DFT coefficients $\breve{a}_i[k]$ can be straightforwardly derived from the functional basis coefficients $\boldsymbol{A}_{i,j}$.

Time-Varying Spectra Time-Varying (TV) spectra attempt to unfold the evolution of the frequency content of the signal over time. While there are several different possible definitions for TV-spectra, the most commonly used in the context of parametric modelling is the "frozen" TV-PSD, in which the instantaneous values of the parameters of the time-variant system are used to calculate the instantaneous PSD as if the system were stationary. Nonetheless, this definition does not relate with practical characteristics of the non-stationary system and can be deemed only as an approximation. In practice, "frozen" spectra are typically characterised by sudden jumps and overall noisy features. Instead, we can use the *Melard-Tjosteim* Time-Variant Spectrum (MT-PSD), which corresponds to the magnitude squared of the inverse DFT of the Harmonic-FRF, as defined below [13, Ch. 4]:

$$S_{MT}(t,\omega) = \sigma_w^2 \cdot \left| \mathcal{F}^{-1}_{\Omega\to t}\{\breve{H}(\omega,\Omega)\} \right|^2 \tag{12}$$

where $\mathcal{F}^{-1}_{\Omega\to t}\{\cdot\}$ indicates the inverse DFT, mapping the frequency variable Ω to time t. The MT-PSD enjoys the nice interpretation as the squared amplitude of the response of the non-stationary (time-periodic) system to a sinusoidal excitation of frequency ω.

3 RESULTS AND DISCUSSION

3.1 Experimental set up

Vibration data are obtained from a SpectraQuest drivetrain simulator, designed as a platform for evaluation of damage diagnosis algorithms in the context of condition monitoring, as shown in Figure 1. The drivetrain simulator characterised by three shafts and two speed reduction gearboxes; a single two-stage parallel-axis gearbox and a single one-stage planetary gearbox. In total, seven accelerometers (sensitivity of $\sim$ 100 mV/g and a 50 g measurement range) are positioned, as depicted in Fig. 1. **Bearings:** Two accelerometers at each of the Bearings 1 & 2 placed on the horizontal and vertical axes (B1-H, B1-V, B2-H and B2-V), mounted on the side and the top of the bearing, respectively, and one accelerometer at Bearing 3 (B3-H) on the horizontal axis mounted on the side. **Gearboxes:** One accelerometer is mounted on the output shaft (MSS side) of the Parallel axis Gearbox, and one accelerometer is placed at the Planetary gearbox towards the output shaft (LSS side), over the ring. All the signals are collected and digitised synchronously with a pair of National Instruments Data Acquisition modules NI-9234, using a sampling rate of 5 120 Hz, 24-bit resolution over a period of 30 minutes.

3.2 Analysed Signal

The analysis presented below corresponds to the pair of signals measured on Bearing 1 in the horizontal and vertical directions (B1-H and B1-V). In the current analysis, we consider the drivetrain response with the HSS is set at 12 rpm and 20% load. LSS is used as reference shaft. Raw signals are down-sampled to 512 Hz and 10 000 samples are extracted for LPV-VAR modelling. The analised signals are displayed in Fig. 2. In the top frame, the reference LSS

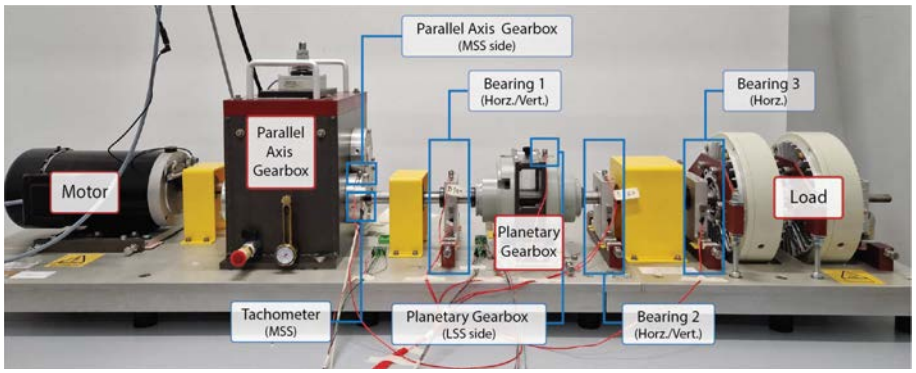

Figure 1: Wind turbine drivetrain diagnostics simulator used in the analysis

angle signal derived from the tachometer is displayed. In the middle frame, the corresponding vibration responses, in the horizontal and vertical directions, are shown. The vibration in the horizontal direction has larger amplitude, due to the increased flexibility of the base in this direction, compared to the vertical. An amplitude modulation pattern is also evident, and seems to correspond with the LSS angle. In the bottom frame, the respective Welch PSD estimates of the raw vibration signals are provided. The Welch PSD estimates are calculated using Hann window with blocksize of $2^{12} = 4096$ samples and 75% overlap. The spectra are dominated by the harmonics of the HSS speed ($\times 12$ Hz), while a vast amount of other harmonics are also present. Detailed analysis (not presented here) indicates that these are related to the LSS speed.

3.3 Model structure selection

The raw vibration signal pair shown in Fig. 2 are used directly to build the LPV-VAR model, together with the LSS angle signal as scheduling variable. LPV-VAR models with a Fourier basis are used to represent the response signal pair. Model structures are assessed in a grid of values for model orders $n_a = 1, 2, \ldots, 80$, and Fourier basis orders $p_a = 1, 2, \ldots, 13$. The fast QR-decomposition algorithm displayed in Tab. 1 is used to calculate and assess all the model structures in the grid of n_a and p_a values. The results, in terms of RSS/SSS, Bayesian Information Criterion (BIC), Samples Per Parameter (SPP) and Condition Number (CN) are shown in Fig. 3a. In parallel, a frequency stabilisation diagram based on the *Best-Linear-Time-Invariant* (Best-LTI) approximation[3] derived from LPV-VAR models with fixed $p_a = 7$ and $n_a = 1, \ldots, 80$, is shown in Fig. 3b. The RSS/SSS and BIC indicate that the predictive performance of the model tends to stabilise for orders over $n_a = 50$. Incremental basis orders also have a positive effect in the model fitness. The SPP and CN figures indicate that the results in the whole grid of values are numerically reliable. In parallel, the frequency stabilisation diagram shows that the LPV-VAR model can accommodate most of the main resonances in the vibration response with model orders over 50, confirming the results seen in the fit criteria. Following from these results, the best LPV-VAR model structure is selected as $n_a = 63$, $p_a = 7$. The selected model structure yields an RSS/SSS of 1.32% (horizontal) and 1.90% (vertical).

[3]The Best-LTI approximation derived from an LPV-VAR model corresponds to the VAR model obtained with the constant basis coefficients of the LPV-VAR model, namely $\boldsymbol{y}[t] = \sum_{i=1}^{n_a} \boldsymbol{A}_{i,1}\boldsymbol{y}[t-i] + \boldsymbol{\varepsilon}[t]$.

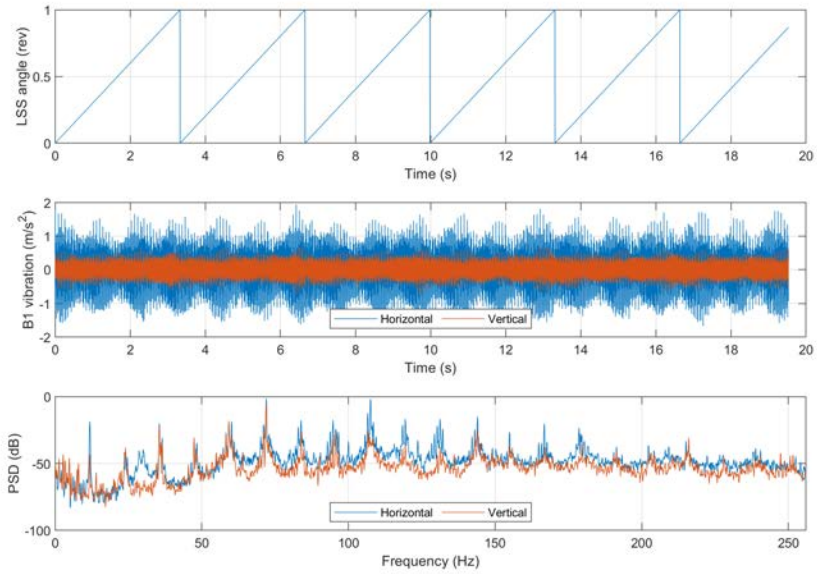

Figure 2: Drivetrain vibration signal pair measured at position B1 in horizontal and vertical directions used for LPV-VAR model structure selection. Top: LSS angle; middle: vibration time series; bottom: vibration PSD estimates (Hann window, blocksize 2^{12} samples, overlap 75%.)

3.4 Model based analysis

A detailed analysis of the drivetrain vibration response dynamics is now performed based on the obtained LPV-VAR model structure, with $n_a = 63$ and $p_a = 7$. The analysis performed below concerns only to the B1-H signal. The LPV-VAR model based Harmonic-FRF evaluated of the horizontal vibration signal in the whole frequency range of the signal (0-252 Hz) for the main and first two cyclic frequencies, together with the scaled PSD estimate, are presented in Fig. 4a. The main component $\breve{H}_0(\omega)$ properly captures the main characteristics of the PSD, consisting on the harmonics of the HSS speed (12 Hz) and structural resonances. Moreover, the harmonics at $\breve{H}_{-2}(\omega)$ to $\breve{H}_2(\omega)$ explain the side-bands around the main harmonics. This is further evidenced in the detailed plot in the frequency range 40-80 Hz, shown in Fig. 4b. Higher order harmonics (not displayed in the plot), represent further details of the main harmonics.

Fig. 5 presents a comparison of time-dependent spectra of the B1-H signal calculated using the spectrogram (Fig. 5a) and the estimated LPV-VAR model (Fig. 5b). The spectrogram is calculated using a sliding Gaussian window of 1024 samples, with an overlap of 1020 samples. The MT-PSD is calculated directly from the inverse DFT of the Harmonic-FRF, as suggested in Eq. (12). While both estimators provide consistent information on the dynamics of the drivetrain signal, the MT-PSD reveals further detail on the evolution of the amplitude/frequency modulation characteristics of the response signal. Likewise, the effect of estimation noise is eliminated in the MT-PSD, particularly in low-power areas in the spectrum. This feature, from a condition monitoring perspective, could facilitate the detection of feeble signal components related to early stages of damage.

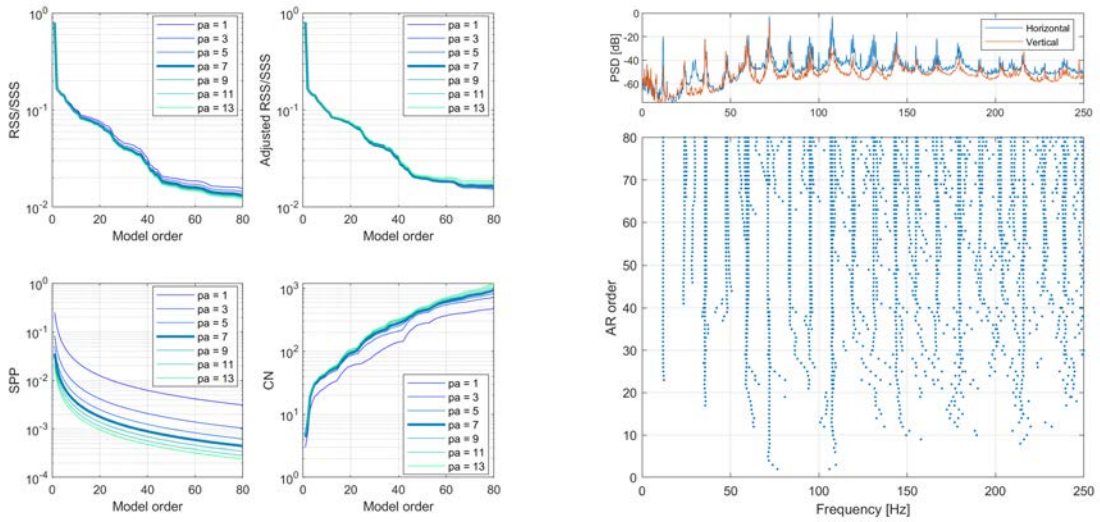

(a) (b)

Figure 3: LPV-VAR model structure selection results for the drivetrain signal measured at position B1, with HSS set to 12 rpm and 20% load. (a) Fit criteria evaluated for different values of n_a and p_a. (b) Frequency stabilisation diagram based on the Best-LTI approximation derived from obtained LPV-VAR models with $p_a = 7$.

4 CONCLUSIONS

This work has been devoted to the short-term modelling of the vibration response of wind turbine drivetrains using LPV-VAR models. These models make use of a reference shaft speed as scheduling variable to represent the cyclo-stationary dynamics of the response signals. While the complexity of these signals calls for highly complex models, we provide a computationally efficient procedure to select the model structure. As a result, we demonstrate that it is possible to construct such high-complexity models with sufficient statistical reliability and providing high-fidelity and accurate representation of the short-term cyclo-stationary dynamics of drivetrain vibration response. An upcoming publication addresses the problem of global modelling, where we consider the response of the structure through a range of operational points. In that context, the LPV-VAR models constructed here form the basis for the global model.

References

[1] T. Wang, Q. Han, F. Chu, and Z. Feng, "Vibration-based condition monitoring and fault diagnosis of wind turbine planetary gearbox: A review," *Mechanical Systems and Signal Processing*, vol. 126, pp. 662–685, 2019.

[2] M. Tiboni, C. Remino, R. Bussola, and C. Amici, "A review on vibration-based condition monitoring of rotating machinery," *Applied Sciences*, vol. 12, p. 972, 2022.

[3] R. B. Randall, *Vibration-Based Condition Monitoring : Industrial, Aerospace and Automotive Ap-*

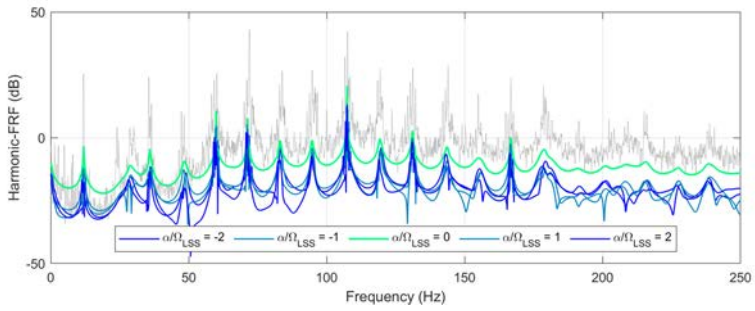

(a)

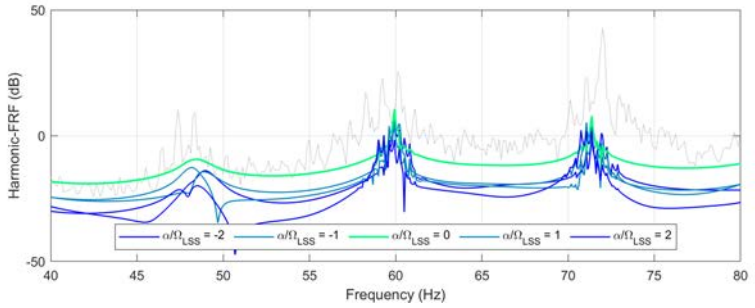

(b)

Figure 4: Harmonic-FRF magnitude of the B1-H signal evaluated on the main and first two cyclic frequencies, derived from the estimated LPV-VAR model. (a) Full frequency range; (b) detail on the frequency range from 40 to 80 Hz. In both plots, the scaled Welch PSD estimate is displayed in the background.

plications. Hoboken: John Wiley & Sons, 2011.

[4] R. Lu, P. Borghesani, R. B. Randall, W. A. Smith, and Z. Peng, "Removal of transfer function effects from gear vibration signals under constant and variable speed conditions," *Mechanical Systems and Signal Processing*, vol. 184, p. 109714, 2023.

[5] A. Stetco, F. Dinmohammadi, X. Zhao, V. Robu, D. Flynn, M. Barnes, J. Keane, and G. Nenadic, "Machine learning methods for wind turbine condition monitoring: a review," *Renewable Energy*, vol. 133, pp. 620–635, 2019.

[6] Z. Chen, A. Mauricio, W. Li, and K. Gryllias, "A deep learning method for bearing fault diagnosis based on Cyclic Spectral Coherence and Convolutional Neural Networks," *Mechanical Systems and Signal Processing*, vol. 140, p. 106683, 2020.

[7] C. Velandia-Cardenas, Y. Vidal, and F. Pozo, "Wind turbine fault detection using highly imbalanced SCADA data," *Energies*, vol. 14, p. 1728, 2021.

[8] L. D. Avendaño-Valencia, E. N. Chatzi, and S. D. Fassois, "In-operation wind turbine modal analysis via LPV-VAR modeling," in *Rotating Machinery, Hybrid Test Methods, Vibro-Acoustics & Laser Vibrometry, Volume 8. Conference Proceedings of the Society for Experimental Mechanics Series*, D. Di Maio and P. Castellini, Eds. Cham: Springer, 2017, pp. 47–57.

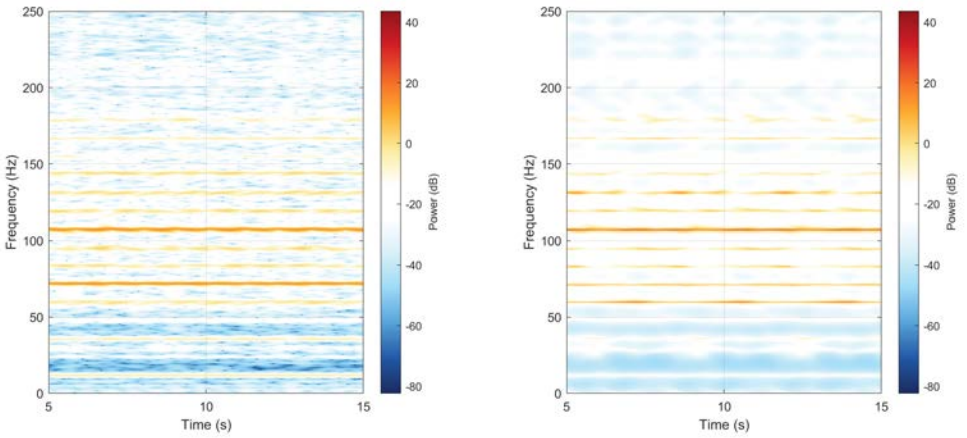

Figure 5: TV spectra derived from the vibration response signal from sensor B1-H. (a) Spectrogram (Gaussian window, blocksize 1024 samples, 1020 samples overlap), (b) *Melard-Tjosteim* TV-spectrum based on the estimated LPV-VAR model.

[9] L. D. Avendaño-Valencia and E. N. Chatzi, "Multivariate GP-VAR models for robust structural identification under operational variability," *Probabilistic Engineering Mechanics*, vol. 60, p. 103035, 2020.

[10] A. B. Jambersi, S. da Silva, and J. Antoni, "Data-driven identification of rotating machines using ARMA deterministic parameter evolution in the angle/time domain," *Journal of the Brazilian Society of Mechanical Sciences and Engineering*, vol. 42, p. 478, 2020.

[11] Y. Chen, M. Rao, K. Feng, and G. Niu, "Modified varying index coefficient autoregression model for representation of the nonstationary vibration from a planetary gearbox," *IEEE Transactions on Instrumentation and Measurement*, vol. 72, pp. 1–12, 2023.

[12] Y. Li, Z. Luo, F. He, Y. Zhu, and X. Ge, "Modeling of rotating machinery: A novel frequency sweep system identification approach," *Journal of Sound and Vibration*, vol. 494, p. 115882, 2021.

[13] L. D. Avendaño-Valencia, "Non-stationary time-dependent ARMA random vibration modeling, analysis & SHM with wind turbine applications," Ph.D. dissertation, Department of Mechanical Engineering and Aeronautics, University of Patras, Patras, Greece, 2016.

[14] P. E. Rossi, G. M. Allenby, and R. McCulloch, *Bayesian Statistics and Marketing*. John Wiley & Sons, 2012.